

# OPENCITY: A SCALABLE PLATFORM TO SIMULATE URBAN ACTIVITIES WITH MASSIVE LLM AGENTS

**Anonymous authors**

Paper under double-blind review

## ABSTRACT

Agent-based models (ABMs) have long been employed to explore how individual behaviors aggregate into complex societal phenomena in urban space. Unlike black-box predictive models, ABMs excel at explaining the micro-macro linkages that drive such emergent behaviors. The recent rise of Large Language Models (LLMs) has led to the development of LLM agents capable of simulating urban activities with unprecedented realism. However, the extreme high computational cost of LLMs presents significant challenges for scaling up the simulations of LLM agents. To address this problem, we propose OpenCity, a scalable simulation platform optimized for both system and prompt efficiencies. Specifically, we propose a LLM request scheduler to reduce communication overhead by parallelizing requests through IO multiplexing. Besides, we design a “group-and-distill” prompt optimization strategy minimizes redundancy by clustering agents with similar static attributes. Through experiments on six global cities, OpenCity achieves a 600-fold acceleration in simulation time per agent, a 70% reduction in LLM requests, and a 50% reduction in token usage. These improvements enable the simulation of 10,000 agents’ daily activities in 1 hour on commodity hardware. Besides, the substantial speedup of OpenCity allow us to establish a urban simulation benchmark for LLM agents for the first time, comparing simulated urban activities with real-world data in 6 major cities around the world. We believe our OpenCity platform provides a critical infrastructure to harness the power of LLMs for interdisciplinary studies in urban space, fostering the collective efforts of broader research communities. Code repo is available at <https://anonymous.4open.science/r/Anonymous-OpenCity-42BD>.

## 1 INTRODUCTION

Agent-based models (ABMs) were first introduced to urban studies in the seminal work of Thomas Schelling about 50 years ago Schelling (2006), which ingeniously explained how segregation can emerge as the aggregation of individual choices. Compared to black-box predictive models, ABMs offer the unique advantage of explaining the underlying mechanisms behind aggregated phenomena, *i.e.*, revealing the connections between “micro-motives” and “macro-behaviours.” As a result, ABMs play an important role in many research areas, including computational social sciences, urban planning and public health. The recent advance of Large Language Models (LLMs) have driven the rise of LLM agents Park et al. (2023); Xu et al. (2023), which leverage LLM’s remarkable capabilities of commonsense reasoning and role-playing to simulate human behaviours. Unlike previous rule-based agents, these emerging LLM agents generate far more realistic human behaviours Park et al. (2023); Shao et al. (2024), and can also explain their inner motives via prompting techniques like chain-of-thoughts Wei et al. (2022). Therefore, LLM agents hold great potential to harness the power of language models in transforming urban studies.

Despite this promising outlook, LLM agents also face severe challenges of scaling up due to the high computation time. In the pioneering work of Park et al. Park et al. (2023) only 15 LLM agents were employed to simulate a small village. One main reason is the prohibitive simulation time, which can be broken down into two parts: on one hand, LLMs are inherently slow due to their enormous model sizes; on the other hand, powerful commercial LLMs are only accessible via APIs, which introduces significant time delay due to network transmission, further slowing down simulation. To make matters worse, the prompt design of urban LLM agents often involve dynamic elements, such

054 as the changing memories and perceived environment Park et al. (2023); Shao et al. (2024). This  
055 important feature prevents the straightforward reuse of simulated behaviors from a small sample of  
056 the population Chopra et al. (2024), as LLM agents need to maintain independent memories and  
057 experiences, which are essential for simulating a vibrant and diverse urban population.

058 In this paper, we present OpenCity, a scalable platform that introduces both system-level and  
059 prompt-level optimizations to enable efficient LLM agent simulation in urban environments. Specif-  
060 ically, we design an LLM request scheduler that leverages the scalable I/O event notification mech-  
061 anism in operating system (*e.g.*, epoll in Linux Bruguera i Moriscot (2019)) to minimize network  
062 transmission delay. This design is based on our key observation that sending LLM requests and  
063 receiving generated output account for only a small portion of total communication time, while the  
064 rest are wasted on waiting for LLM responses and the repeatedly establishing TCP connections Pe-  
065 terson & Davie (2007). To address this problem, the LLM request scheduler uses the scalable I/O  
066 event notification mechanism to parallelize LLM requests by reusing the network I/O portal and  
067 TCP connections while waiting for responses. Besides, LLM request scheduler also analyzes the  
068 interdependencies of LLM requests and local computation tasks, *e.g.*, updating agent’s memory and  
069 retrieving nearby locations, ensuring local computation tasks are optimally distributed across mul-  
070 tiple CPU cores. These system-level optimizations enable large-scale LLM agent simulations to  
071 run on commodity hardware. As for the prompt-level optimization, OpenCity introduces a novel  
072 “group-and-distill” prompt strategy to minimize the input token required by LLMs. The key idea  
073 is to identify the clusters of LLM agents that share semantically similar static elements, *e.g.*, age,  
074 gender and income level, and use shared context in batch prompting Cheng et al. (2023) to reduce  
075 token redundancy. Specifically, our “group-and-distill” strategy leverages the in-context learning  
076 capabilities of LLMs to implement a prototype learning workflow that automatically discovers clus-  
077 ters of LLM agents with semantically similar static elements for simulation. Agents within the same  
078 clusters are grouped into a batch prompt, and we design a “prompt distillation” to extract shared  
079 prefix for grouped agents. Finally, OpenCity also features an easy-to-use web portal that facilitates  
080 code-less simulation configuration and result visualization. This design minimizes the program re-  
081 quirement for running simulation with LLM agents, ensuring our OpenCity platform can benefit  
082 researchers from all background.

082 We evaluate the efficiency and faithfulness of OpenCity in simulating the urban activities of 6 cities  
083 around the world using the widely adopted Generative Agent workflow Park et al. (2023). Our ex-  
084 periments show OpenCity achieves an average 635x acceleration in simulations with 10,000 LLM  
085 agents. Besides, the number of requests and consumed tokens are reduced by 73.7% and 45.5%, re-  
086 spectively. OpenCity also shows strong scalability, with the simulation time per agent reducing from  
087 36.25 to 0.06 seconds as the simulation size increases from 1 to 10,000 agents, demonstrating that  
088 larger simulations allow for more efficient LLM request scheduling and prompt distillation. More  
089 importantly, OpenCity also maintains high faithfulness of the simulated behaviour. Specifically,  
090 the Jensen–Shannon divergence and top-1 hit rates of our method are comparable to the standard  
091 prompting technique of batch prompting Cheng et al. (2023), and substantially surpass straightfor-  
092 ward reusing strategy Chopra et al. (2024). Besides, the top-1 hit rate can reaches up to 96% when  
093 using powerful LLMs like GPT-4o.

094 The substantial simulation acceleration allows us to benchmark LLM agents’ ability to replicate  
095 large-scale urban activities for the first time. We use classic evaluation measures such as the radius  
096 of gyration Gonzalez et al. (2008), origin-destination matrix Jiang et al. (2016), and segregation  
097 index Moro et al. (2021) to assess LLM agents’ simulations. These are the most widely adopted  
098 metrics that characterize urban residents’ activities at both individual and group levels, and across  
099 physical and social domains. Our experiments show that LLM agents perform comparably to, or  
100 better than, traditional rule-based agents like EPR Song et al. (2010). Moreover, LLM agents enable  
101 counterfactual analyses, such as evaluating experienced segregation in cities without residential seg-  
102regation Massey & Denton (1988). They also allow researchers to interrogate LLM agents’ motives  
103 behind their behaviors, offering valuable insights for urban policy-making.

103 The contribution of this paper are three-folds:

- 105 • We design a high-performance platform OpenCity that introduces system-level LLM re-  
106 quest scheduler and prompt-level “group-and-distill” strategy to reduce LLM agent simu-  
107 lation time. OpenCity maintains high fidelity in simulated behaviors while achieving an  
average 635x acceleration.

- The substantial speedup allows us to benchmark LLM agents for reproducing urban activities for the first time.
- OpenCity provides a user friendly web portal, allowing researchers without programming background to easily configure simulation and visualize the results.

## 2 RELATED WORKS

### 2.1 LLM AGENTS

With the widespread use of large language models (LLMs) in various applications, the limitations of LLMs, e.g., unstable reasoning abilities, limited memory capacity, and lack of specialized expertise, have been exposed to the public. As one of the potential solution, LLM agents are proposed to overcome these limitations and promote the practical application of LLMs. AutoGPT Gravitas (2023) as one of the most popular LLM autonomous agent explore the potential of applying LLM to enable the autonomous planning and task-solving. After that, LLM agents Wang et al. (2024); Xi et al. (2023) have made significant progress in two directions: task-oriented agents and simulation agents. Following the first direction, researchers aim to improve LLM agent’s ability to solve complex tasks. For example, lots of programming agents, such as ChatDev Qian et al. (2023), SWEAgent Yang et al. (2024), and MetaGPT Hong et al. (2023), are designed to solve the complex programming tasks. As for the second direction, generative agents Park et al. (2023) have demonstrated the potential of large models in simulating human behavior, which has been further validated in subsequent research. S3 Gao et al. (2023) explores the potential of using LLM agents to simulate the social network. CoPB Shao et al. (2024) defines a agentic workflow to simulate the mobility behaviors. RecAgent Wang et al. (2023) simulate the user behavior in the recommendation system. While these works demonstrate the potential of LLM agents, the large scale efficient simulation of generative agents becomes the critical bottleneck of further applications.

### 2.2 LLM DEPLOYMENT OPTIMIZATION

To support the efficient inference of LLMs and LLM agents, enormous works and systems Miao et al. (2023) are designed to optimize the inference efficiency of LLMs and further accelerate their practical applications. For example, Flash-attention Dao et al. (2022) is an IO-aware exact attention algorithm which uses tiling to reduce the number of memory reads/writes within GPU. AWQ Lin et al. (2024) is an activation-aware weight quantization to compress and accelerate the LLM inference. vLLM Kwon et al. (2023) proposes pagedAttention mechanism to enable highly efficient KV cache scheduler during the inference and becomes the most population open source LLM inference engine. SGLang Zheng et al. (2023) provides a flexible frontend language to enable the efficient autonomous optimization of LLM inference. While these systems are designed to process the general LLM inference, specific characteristics of generative agents especially urban generative agents are ignored which can be employed to further accelerate the inference and simulation. In this paper, we explore the potential of this direction and design the OpenCity platform.

## 3 PRELIMINARIES

### 3.1 LLM AGENTS FOR URBAN ACTIVITIES

We focus on using LLM agents to reproduce urban dynamics characterized primarily by physical mobility. Consider an urban environment  $E$  containing  $N$  LLM agents. The state of agent  $i$  at simulation time  $t$ , denoted as  $S_i(t) = \{s_i, m_i(t)\}$ , consists of both static properties  $s_i$  and dynamic properties  $m_i(t)$ . Static properties, like the agent’s demographics, remain constant throughout the simulation, while dynamic properties, such as memory and perceived environment information, change frequently and are hard to predict. We can represent the state update of agent  $i$  using a function  $f$ :

$$m_i(t+1) = f(s_i, E, m_i(t); S_i(t+1) = \{s_i, m_i(t+1)\}) \quad (1)$$

Here,  $m_i(t+1)$  is the updated memory of agent  $i$  at time  $t+1$ , and the function  $f$  models how the agent updates its state by perceiving the urban environment  $E$ , reflecting on its memory  $m_i(t)$ ,

162 and interacting with the LLM. The individual trajectory of agent  $i$ , denoted as  $T_i$ , describes the  
 163 trajectory of the agent over time in the urban environment  $E$ . If the location of agent  $i$  at time  $t$  is  
 164 represented by  $L_i(t)$ , which depends on its state  $S_i(t)$ , then the individual trace can be expressed  
 165 as  $T_i = \{L_i(0), L_i(1), L_i(2), \dots, L_i(t_s)\}$ , where  $t_s$  is the total simulation time. Along with  
 166 individual mobility, we also examine the aggregated mobility features  $A = \Phi(\sum_i \phi(\sum_t S_i(t)))$ ,  
 167 such as Original-Destination (OD) matrix and income segregation index, which reflects the urban  
 168 dynamics involving states of all agents.

169 To simulate LLM agents in the urban space, we set the initial state for the agents and environment  
 170  $\{S_i(0)|i \in N\}$  and then apply the Equation 1 for each agent at every simulation step. When the  
 171 number of agents increases, challenges arise mainly because of the LLM request process. LLMs  
 172 are inherently slow due to their parameter size, and when using commercial LLMs accessed via  
 173 APIs, response times can be further delayed, especially with poor network conditions. Some have  
 174 proposed reusing the LLM response for agents can improve the efficiency Chopra et al. (2024), but it  
 175 requires that the agents have the completely same state or have limit kinds of state that can be easily  
 176 predicted. What’s more, simply reusing the response would eliminate the independence of agents  
 177 and reduce the faithfulness of the simulation results. Urban agent  $i$  has dynamic memory  $m_i(t)$   
 178 that evolves during the simulation. This memory  $m_i(t)$  depends not only on past memory  $m_i(t_h)$   
 179 but also on the current environment. Since decision-making and memory updates rely heavily on  
 180 the LLM, predicting an agent’s future state or finding an agent with an identical state to reuse an  
 181 LLM response is difficult. Therefore, to simulate the large-scale and reliable LLM agents for urban  
 182 dynamics, a simple response reuse strategy is insufficient.

### 183 3.2 TIME COST ANALYSIS

184  
 185 In light of the prevailing dominance of remote LLM service invocations in the current operational  
 186 landscape of LLM agents simulation, a decomposition of the time required for a single LLM request  
 187 can be undertaken, as illustrated in Fig.1(b). The first phase is the initialization and reception time for  
 188 the LLM request, the second is the TCP/IP connection and destruction time between the simulation  
 189 system and the LLM service provider, and the third is the data transmission and waiting time. For a  
 190 single LLM request, the overhead of the first and second phases is relatively low in comparison to  
 191 the third, and the core time consumption is derived from the data transmission and waiting.

192 The simulation of large-scale agents necessitates the issuance of a considerable number of LLM  
 193 requests, which, given the presence of waiting periods, impairs the overall efficiency of the simulator.  
 194 Furthermore, the system resources are not fully utilized. Consequently, the effective scheduling  
 195 of LLM requests is essential for enhancing the overall utilization of system resources, which in  
 196 turn improves the overall efficiency of the simulation. Furthermore, as the time required for LLM  
 197 inference is directly proportional to the number of tokens contained in an LLM request, it is also  
 198 important to reduce the number of tokens consumed per agent while compressing the number of  
 199 requests.

200 From this vantage point, the present work puts forth an efficacious LLM request scheduler and a  
 201 prompt distillation method, which can markedly enhance the efficiency of large-scale LLM agents  
 202 simulation.

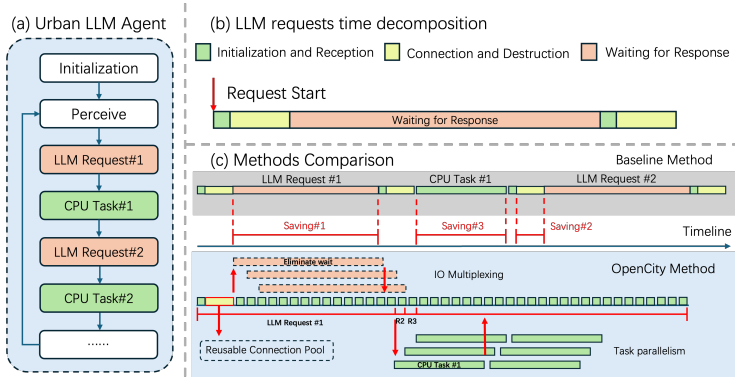
## 204 4 OPENCITY PLATFORM

205  
 206 We devise a scalable platform OpenCity to accelerate the simulation of urban LLM agents from  
 207 both system- and prompt-level. The OpenCity platform aims to substantially reduce the simulation  
 208 time per LLM agent while maintaining high simulation fidelity. Besides, OpenCity also provides a  
 209 user-friendly web interface to facilitate the easy access of researchers from diverse background. The  
 210 key designs are introduced as follows.

### 212 4.1 LLM REQUEST SCHEDULER

213  
 214 As shown in Fig.1(a), for a LLM agent, the dependency between its LLM requests—that is, the  
 215 necessity for the next LLM request to be initiated after the previous one is completed—results in  
 a constant waiting time under the condition of a fixed network environment and request content.

216 In contrast, for a system comprising multiple agents, there is no dependency between their LLM  
 217 requests. In order to achieve asynchronous processing of multiple LLM requests, we have imple-  
 218 mented an IO multiplexing scheme (based on epoll in Linux) which eliminates waiting time in the  
 219 simulation system. This allows the operating system to manage IO waiting, thereby achieving the  
 220 desired "zero-awareness" of data transmission in the simulation system. Consequently, the aver-  
 221 age time for a LLM request is reduced to the time required for the first and second phases (Time  
 222 saving#1 in Fig.1(c)).



224 Figure 1: The functionality of the proposed LLM Request Scheduler.

236 Furthermore, the considerable number of LLM calls necessitates the frequent establishment of con-  
 237 nections with the service provider, resulting in a considerable overhead in the establishment and  
 238 destruction of each connection. However, given that the content of LLM requests is inherently  
 239 linked to the corresponding agent, it is possible to leverage the same connection for multiple agents,  
 240 thereby reducing the overall performance overhead. To address this issue, a pool of reusable connec-  
 241 tions is maintained within the system. Upon initiation of an LLM request by an agent, the request  
 242 content is populated into an available connection, thus avoiding the establishment of a new connec-  
 243 tion. This approach additionally reduces the mean time consumption of LLM requests (Time  
 244 saving#2 in Fig.1(c)).

247 For those agents with CPU tasks during the computation process, it is important to note that the  
 248 continued occupation of CPU resources by the computation load will inevitably result in a delay  
 249 in the sending of LLM requests from subsequent agents. To mitigate the adverse effects of this  
 250 issue on the system’s overall performance, we categorize the CPU task as "local IO", offload it to  
 251 available cores for computation through a multi-core parallel scheme, and then return the result to  
 252 the designated agent upon completion of the computation. This approach further ensures the stable  
 253 operation of asynchronous LLM requests (Time saving#3 in Fig.1(c)).

254 The proposed LLM request scheduler is designed to reduce the waiting time for a significant number  
 255 of LLM requests during the simulation runtime. Based on the supporting auxiliary scheme, it has  
 256 the potential to significantly enhance the efficiency of large-scale LLM agents.

258 4.2 GROUP-AND-DISTILL META-PROMPT OPTIMIZER

260 A further crucial method for enhancing the efficiency of the simulation is to reduce the number of  
 261 LLM requests issued by agents and the quantity of tokens consumed by said agents. A conventional  
 262 approach is to reuse the generated result of a single LLM request across multiple agents. However,  
 263 this approach presents two significant drawbacks: 1. In fine-grained urban LLM agent simulations,  
 264 each agent possesses its own dynamic properties. Consequently, the reuse scheme compromises  
 265 the independence of agents, which is antithetical to the objective of conducting urban simulations  
 266 through large-scale LLM agents. Furthermore, for agents with dynamic properties, it is inherently  
 267 impossible to share the result of a single LLM request, as shown in Fig.2(a).

268 To address this issue, we propose the Group-and-Distill Meta-Prompt Optimizer (depicted in Fig.2),  
 269 which employs group information in lieu of the static attributes of the agent. This approach aggre-  
 gates requests from multiple agents at runtime and realizes prompt by sharing group information and

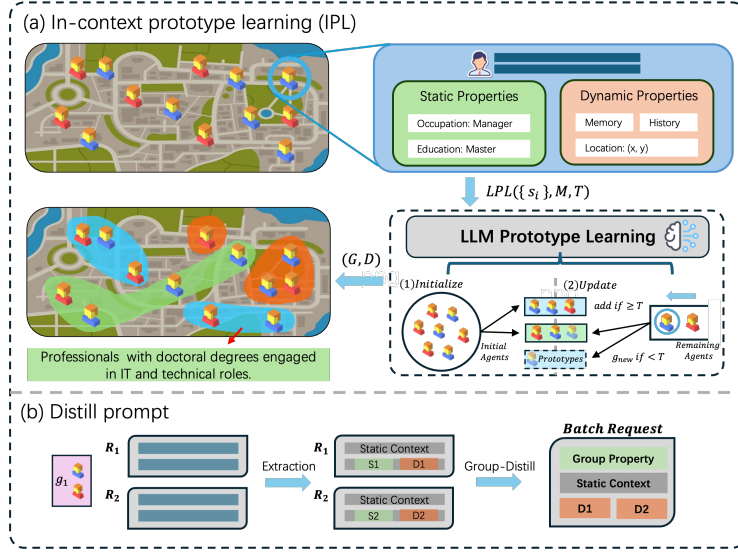


Figure 2: Overview of Group-and-Distill Meta-Prompt Optimizer.

context information while preserving the agent’s dynamic properties. The optimizer is comprised of two distinct components. In-context prototype learning (IPL) and distill meta-prompt.

The inputs and outputs of IPL are defined as follow:

$$IPL(\{s_i\}, M, T) \rightarrow \mathbf{G}, \mathbf{D} \quad (2)$$

in which,  $\{s_i\}$  is the collection of agent’s static properties;  $M$  controls the number of agents in initial prototype learning;  $T$  is the threshold for decision making;  $\mathbf{G}$  is the collection of agent groups;  $\mathbf{D}$  is the descriptions for each group of agents.

Input the static properties of a set of agents, IPL first groups the first  $M$  agents, providing both group results and the corresponding description information. Subsequently, IPL classifies the remaining agents by transmitting the static properties of the agent to LLM, which analyzes the likelihood of the agent belonging to each group based on the group description and provides the quantization result. By comparing the quantization result with  $T$ , when the result is greater than  $T$ , IPL assigns the agent to the specified group. Otherwise, it constructs a new group and describes the characteristics of the group. In comparison to conventional prototype learning methods that operate within a fixed parameter space, IPL exhibits enhanced generalization capabilities and a particular aptitude for leveraging semantic-level knowledge in the prototyping process. The prototype information obtained by IPL is employed to efficiently summarize the static attribute characteristics of the set of agents within the specified group.

The distill meta-prompts obtained through a systematic examination of the original prompts and the CoT approach is employed to generate the prompts (details can be found in Fig.A1). To facilitate the generation procedure, we have proposed a raw prompt design diagram, which divides the prompt into three sections: the function section, the variable section, and the input section. The generation process, which is initiated with a given raw prompt, comprises four steps: summarization, context extraction, information sharing, and rewriting of the raw prompt into the distill meta-prompt. In the operational phase, the requests from the agents in a group are aggregated into a single Distill request, which has the effect of reducing the number of LLM requests and the consumption of tokens.

The proposed prompt optimizer enables further enhancement of simulation efficiency and reduction of simulation cost while maintaining agent dynamic properties.

### 4.3 WEB PORTAL

A web portal has been designed for the utilisation of OpenCity, encompassing the frontend, backend, and simulation system. This enables users to rapidly configure simulation conditions and visualise

simulation results, as well as facilitating the storage of simulation data and urban infrastructure information within a database. The fundamental concept underlying the design of this portal is user-friendliness, particularly given the inherently interdisciplinary nature of urban research. We have developed a rapid, code-free configuration approach tailored to the needs of researchers, thereby facilitating the seamless engagement of experts from diverse fields with our simulation platform.

**User-friendliness:** In order to enhance the usability of the OpenCity platform, the Web Portal has been augmented with the incorporation of the LLM agent blueprint construction function. Users are able to drag and drop each basic function module in order to construct complex logic for LLM agents. In order to meet a variety of needs, the blueprint function is based on the established LLM agent development frameworks, such as Langchain Pandya & Holia (2023) and AutoGPT Yang et al. (2023), and incorporates several fundamental modules oriented towards urban simulation, including environmental and traffic sensing. The blueprint offers an efficient and agile development solution for interdisciplinary researchers, facilitating the rapid iteration of simulation methods and theories.

**Basic workflow:** The primary process of urban LLM agent simulation on this web portal is comprised of three distinct phases: citizen profile configuration, deployment and simulation, and results presentation. The configuration of the citizen profile is facilitated by the provision of a console hub, which enables users to efficiently and transparently administer the simulation tasks they have created on the platform, along with the agents within those simulations. The user is able to bind the execution logic designed in the blueprint to different agents and to configure their profiles with great rapidity via the web interface. This may entail selecting a city, selecting an existing profile, or filling out a profile manually. Once the configuration process is complete, users can deploy and initiate simulations on the platform with a single click, leveraging the backend system and simulation system. The web portal also offers a monitor page, which enables users to observe the real-time outcomes of ongoing simulations and assess the performance of their agents. Finally, after the simulation has concluded, users can access the portal to view macroscopic statistical results in a visual format, such as Origin-Destination (OD) maps. An exemplar of the proposed web portal in operation can be found in Figure A2.

## 5 BENCHMARK

### 5.1 DATASET AND SETUP

**Dataset** We collect urban mobility data in 6 major cities around world: Beijing, New York, San Francisco, London, Paris, and Sydney. The data sources vary. Beijing’s data comes from a related work Shao et al. (2024), which collected from social network platform. New York and San Francisco source from Safegraph for aggregated population flow data. And the other three cities are from Foursquare which consist of thousands of check-ins data. To make better use of these data, we have done some preprocess method, such as trajectory filter, home extraction and profile sampling. More details can be seen in Appendix A.

**Architecture of LLM Agent** The main agent used in OpenCity platform to simulate the urban dynamic is the generative agent Park et al. (2023). Generative agents use a framework that involves perception, planning, and reflection. A generative agent first creates a daily plan to ensure the trajectory is reasonable. When the agent arrives at a POI, it makes decisions based on current perceptions and memory. After taking action, the agent records the action and the POI into its memory stream. Once the memory stream reaches a threshold, the agent reflects. The results show that the generative agent to function well in the OpenCity platform.

We also have rule-based agent for comparison, such as the famous Explore and Preferential-Return (EPR) model Song et al. (2010). This work make agent choose to explore a new location or return to the visited location. Decisions are related to some parameters to compute the probability. In this paper, we set the parameters as follows: exploration rate  $\rho = 0.6$ , exploration-return trade-off parameter  $\gamma = 0.21$ , waiting time distribution parameters  $\tau = 17, \beta = 0.8$ .

### 5.2 ACCELERATION PERFORMANCE

This section presents an evaluation of the performance of the OpenCity platform in conjunction with the Generative Agent (Tested on Huawei ECS Cloud Server - Intel(R) Xeon(R) Platinum 8378C

CPU @ 2.80GHz with 64 cores and 256 GB RAM). The performance of the platform was evaluated in six major cities with 10,000 agents. The results are presented in Table.1, where the following variables are defined: *Speedup* denotes the improvements in simulation time, *Rr* denotes the LLM request number reduction rate, and *Tr* denotes the token number reduction rate.

The results demonstrate that OpenCity exhibits substantial acceleration in all test cities, with an average runtime of 0.058s per LLM agent and an average speedup of 635.3x in simulation time. Furthermore, the proposed acceleration scheme is capable of markedly reducing the number of LLM requests and token consumption, with an average reduction of 73.7% and 45.5%, respectively.

To assess the scalability of OpenCity, we conducted a series of simulations to evaluate its acceleration performance under varying orders of magnitude of agents. The results of this analysis are presented in Fig.3, in which the baseline represents the simulation time without optimization. The results demonstrate that OpenCity’s acceleration capability is scalable, with a notable enhancement in acceleration effect when the number of agents is increased from 10 to 10,000. This is due to the fact that as the number of agents increases, the number of groups obtained based on IPL also gradually increases. This, in turn, allows the advantages of the LLM request scheduler to be fully realised, thereby ensuring a better utilisation of system resources.

Cities	Time	<i>Speedup</i>	<i>Rr</i>	<i>Tr</i>
Beijing	0.07s	521.7	73.2%	38.7%
New York	0.06s	624.7	67.3%	37.6%
San Francisco	0.07s	588.6	80.3%	51.3%
London	0.04s	792.5	74.6%	49.9%
Paris	0.06s	640.0	76.3%	48.6%
Sydney	0.05s	644.0	70.7%	46.6%
<b>Average</b>	<b>0.058s</b>	<b>635.3</b>	<b>73.7%</b>	<b>45.5%</b>

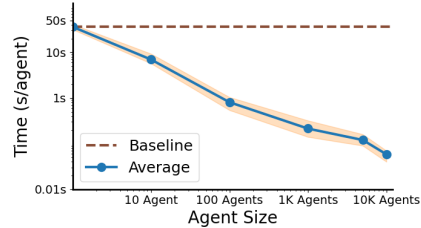


Table 1: Acceleration experiment results

Figure 3: Scalability experiments

Furthermore, faithfulness experiments are conducted to demonstrate that the Group-and-Distill optimizer can effectively preserve the distinctive personality traits of the agents. The testbed for this evaluation is location choice generation, which requires the combination of agent properties to select the next location to visit. A comparison was conducted between the performance of four distinct methods, including raw prompting (without any modification), batch prompting Cheng et al. (2023), archetype prompting Chopra et al. (2024), and the proposed method. One hundred agents were randomly selected and location selection was performed 100 times for each agent with the same context. The effectiveness of the method was evaluated by counting the distribution of selections (*JSD*) as well as the top-1 hit rate (*T1*). The results are shown in Table.2, where Inherent denotes the bias present in LLM itself (raw prompt method).

Model and Cities	Inherent		Batch prompting		Archetype prompting		Ours		
	<i>JSD</i>	<i>T1</i>	<i>JSD</i>	<i>T1</i>	<i>JSD</i>	<i>T1</i>	<i>JSD</i>	<i>T1</i>	
4o-mini	BJ	0.04 ± 0.02	90%	0.11 ± 0.05	76%	0.89 ± 0.04	8%	0.13 ± 0.02	74%
	NY	0.02 ± 0.01	92%	0.07 ± 0.03	81%	0.84 ± 0.11	13%	0.06 ± 0.04	86%
	SF	0.03 ± 0.02	88%	0.09 ± 0.04	77%	0.91 ± 0.03	11%	0.10 ± 0.03	85%
	Lo	0.06 ± 0.04	89%	0.12 ± 0.07	79%	0.86 ± 0.06	9%	0.12 ± 0.04	78%
	Pa	0.05 ± 0.02	86%	0.17 ± 0.11	69%	0.94 ± 0.03	4%	0.14 ± 0.04	71%
	Sy	0.04 ± 0.03	85%	0.08 ± 0.03	75%	0.88 ± 0.05	5%	0.07 ± 0.04	75%
GPT-4o	NY	0.003 ± 0.002	98%	0.012 ± 0.007	94%	0.89 ± 0.09	10%	0.009 ± 0.004	97%
	Pa	0.004 ± 0.002	99%	0.021 ± 0.009	93%	0.91 ± 0.04	7%	0.010 ± 0.006	96%

Table 2: Faithfulness experiment results

As evidenced by the results, our method demonstrates the capacity to maintain a comparable level of consistency to that observed in the batch prompting method, while exhibiting a reduction in volatility and token consumption. However, the archetype prompting method performs poorly in this evaluation, which further demonstrates the inability of the reuse-based method to accommodate the dynamic properties of agents. Furthermore, given the considerable discrepancies observed in the raw prompting method when evaluated using the GPT-4o-mini model, an additional assessment was conducted on two cities, New York and Paris, utilising the GPT-4o model. The findings indicate that our method is capable of approximating the execution of the raw prompting method to a



432 significant degree. Additionally, the results indicate that there are notable discrepancies between dif-  
 433 ferent models in terms of environmental comprehension and the capacity to process lengthy textual  
 434 content. The consistency of LLM outcomes merits further examination.

435 In general, OpenCity is capable of markedly enhancing the efficiency of large-scale urban LLM  
 436 agent simulations while concurrently preserving the distinctive characteristics of the agents them-  
 437 selves. This enables the cost of simulating populations exceeding 10,000 to be maintained at the  
 438 hourly level.

### 440 5.3 REPRODUCING URBAN DYNAMICS

442 The significant increase in simulation efficiency enables us to benchmark LLM agent’s ability to  
 443 reproduce large-scale urban dynamics for the first time. We use comprehensive metrics in three-  
 444 levels to evaluate the simulation performance, from individual- to group level, and also from physical  
 445 domain to social domain. At the individual level, we calculate the radius of gyration Gonzalez et al.  
 446 (2008) for each user. At the group level, we use the original-destination matrix Jiang et al. (2016). As  
 447 for the social domain, we focus on the income segregation index Moro et al. (2021). To evaluation  
 448 the simulation performance, we compute the MSE for these three metrics, which are denoted as  
 449  $R_{MSE}$ ,  $OD_{MSE}$  and  $S_{MSE}$ . More details can be referred to Appendix B.

450 In this section, we analyze the performance of the Generative Agent and EPR Agent in reproducing  
 451 urban dynamics. We test both agents in 6 major cities using 1,000 agents. The results are shown  
 452 in Table 3. The results indicate that both the Generative Agent and EPR Agent successfully re-  
 453 produce urban dynamics with low MSE values. Additionally, the LLM Agent performs as well as  
 454 or better than the classical rule-based EPR Agent, highlighting the advantage of LLM’s semantic  
 455 understanding ability in urban simulations.

457 Cities	458 GenerativeAgent			459 EPR		
	$R_{MSE}$	$OD_{MSE}$	$S_{MSE}$	$R_{MSE}$	$OD_{MSE}$	$S_{MSE}$
460 Beijing	19.5	3.88e-4	0.0312	29.8	4.26e-4	0.0630
461 New York	-	5.95e-4	0.3521	-	3.70e-4	0.2319
462 San Francisco	-	23.6e-4	0.1535	-	14.0e-4	0.0352
463 Paris	2.48	7.58e-4	0.1255	4.04	6.25e-4	0.1240
464 London	6.24	5.22e-4	0.1258	25.7	7.41e-4	0.1501
465 Sydney	15.1	4.71e-4	0.1118	54.2	7.63e-4	0.1265

466 Table 3: Urban dynamics reproduction results

## 468 6 CASE STUDY: EXPERIENCED URBAN SEGREGATION

470 With the ability to simulate large-scale urban LLM agents, we can conduct counterfactual exper-  
 471 iments to explore outcomes under different policies and design optimal strategies for the future.  
 472 Conventional rule-based models do not support this capability, as they are designed to simulate  
 473 real-world scenarios. Experienced urban segregation is a widely discussed issue with significant  
 474 impacts on social dynamics and the economy. It arises from both demographic differences in resi-  
 475 dential neighborhoods and the mobility patterns of urban residents Moro et al. (2021). This section  
 476 provides a case study: a counterfactual simulation is conducted in New York and San Francisco,  
 477 to observe how the simulation results change in different configurations, and try to summarize the  
 478 results with the LLM agents themselves.

479 Specifically, we construct the counterfactual scenario by evenly distributing LLM agents with dif-  
 480 ferent income levels across the city, that means we almost eliminate the residential segregation. The  
 481 results of the income segregation statistics with CBGs as the statistical granularity are shown in  
 482 Fig.4, where ‘Original’ samples the segregation results from the real census data, and ‘Even’ is the  
 483 result after uniform distribution of agents with different incomes.

484 From the results, it can be seen that the segregation of the two cities changed significantly after  
 485 the different income groups were evenly distributed in the cities. In New York City, the mean  
 segregation index decreases from 0.845 to 0.172, and in San Francisco, the mean segregation index

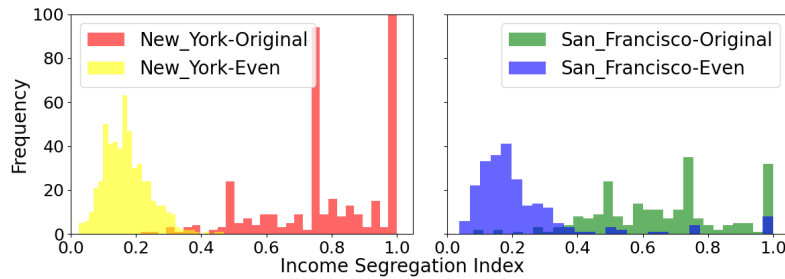


Figure 4: The distribution of income segregation index for counterfactual experiment.

decreases from 0.665 to 0.232. As a result, we believe that differences between regions are the main cause of segregation as opposed to segregation by choice of action. To extend, we can know that with policies that promote more even income distribution among neighborhoods, urban segregation and social inequality can be improved.

Human Input	What places did you go today and why?	How many people did you see today? How were they?
Agent Output	<p>About the places I visited today and the reasons:</p> <ol style="list-style-type: none"> <li>1.Sleep at home (00:00 - 10:00): Resting to start the day.</li> <li>2.Brunch (10:00 - 11:32): Enjoying a leisurely meal.</li> <li>3.Outdoor Activity (12:06 - 14:45): Engaging in physical activity</li> <li>4.Curry Boyz (15:43 - 17:10): Likely for a meal, perhaps trying Indian cuisine.</li> <li>5.Walgreens (17:53 - 20:38): To pick up personal care items or medication.</li> <li>6.Blush! Wine Bar (21:23 - 23:02, and stayed until late): Relaxing, enjoying wine, and possibly socializing.</li> </ol> <p>Each place was chosen for a mix of relaxation, exercise, dining, and socializing.</p>	<p>The people I met today:</p> <ol style="list-style-type: none"> <li>1. When I went to Curry Boyz, I met [547] and [1032], [547] is an IT engineer, [1032] is a teacher, [547] has a high level of consumption, [1032] has a medium level of consumption.</li> <li>2. When I went to Blush! Wine Bar, I met 1032 and 779, [779] is a worker, [779]'s consumption level is slightly low.</li> </ol> <p>The above is about the people I met today and what they were up to.</p>

Figure 5: A detail case of interpreting simulation results through communication.

Furthermore, we use natural language to communicate with those involved agents to gain deeper insights about urban segregation. One detailed case is shown in Fig.5. When we ask an agent about its daily journey, it can accurately provide the time and locations it visited. This is because the agent caches runtime information and uses the LLM’s ability to understand semantic details. When asked about the people it met, the agent lists everyone it encountered at different locations and provides their information. This is due to vectorized storage of the agent’s simulation results and the LLM’s ability to retrieve that information. Collecting and observing fine-grained statistical information through conversations with agents and even through LLM improves both the interpretability of the simulation and our understanding of the simulation goals.

## 7 CONCLUSION

In this work, we introduced OpenCity, a scalable platform designed to address the computational and communication challenges inherent to the deployment of large-scale LLM-based urban agents in city simulations. By incorporating an LLM request scheduler and a novel "group-and-distill" prompt optimization strategy, we achieved a notable 600-fold increase in the efficiency of agent simulations, with a substantial reduction in both LLM requests and token usage. The OpenCity platform was evaluated through experiments conducted on six global cities. The results demonstrated the platform’s capability to simulate the daily activities of 10,000 agents at an hourly level, while also establishing a benchmark for generative agent performance in urban contexts. The platform’s ability to compare simulated behaviors with real-world data highlights its potential for real-world urban-scale applications, offering a robust tool for urban planners and researchers to explore and understand complex societal phenomena.

## REFERENCES

- 540  
541  
542 Francesc Bruguera i Moriscot. Benchmarking input/output multiplexing facilities of the linux kernel.  
543 2019.
- 544 Zhoujun Cheng, Jungo Kasai, and Tao Yu. Batch prompting: Efficient inference with large language  
545 model apis. *arXiv preprint arXiv:2301.08721*, 2023.
- 546  
547 Ayush Chopra, Shashank Kumar, Nurullah Giray-Kuru, Ramesh Raskar, and Arnau Quera-Bofarull.  
548 On the limits of agency in agent-based models. *arXiv preprint arXiv:2409.10568*, 2024.
- 549  
550 Tri Dao, Dan Fu, Stefano Ermon, Atri Rudra, and Christopher Ré. Flashattention: Fast and memory-  
551 efficient exact attention with io-awareness. *Advances in Neural Information Processing Systems*,  
552 35:16344–16359, 2022.
- 553  
554 Chen Gao, Xiaochong Lan, Zhihong Lu, Jinzhu Mao, Jinghua Piao, Huandong Wang, Depeng Jin,  
555 and Yong Li. S<sup>3</sup>: Social-network simulation system with large language model-empowered  
556 agents. *arXiv preprint arXiv:2307.14984*, 2023.
- 557  
558 Marta C Gonzalez, Cesar A Hidalgo, and Albert-Laszlo Barabasi. Understanding individual human  
559 mobility patterns. *nature*, 453(7196):779–782, 2008.
- 560  
561 Significant Gravitas. Autogpt. [https://github.com/Significant-Gravitas/  
562 AutoGPT](https://github.com/Significant-Gravitas/AutoGPT), 2023. Accessed: 2024-09-01.
- 563  
564 Sirui Hong, Xiawu Zheng, Jonathan Chen, Yuheng Cheng, Jinlin Wang, Ceyao Zhang, Zili Wang,  
565 Steven Ka Shing Yau, Zijuan Lin, Liyang Zhou, et al. Metagpt: Meta programming for multi-  
566 agent collaborative framework. *arXiv preprint arXiv:2308.00352*, 2023.
- 567  
568 Shan Jiang, Yingxiang Yang, Siddharth Gupta, Daniele Veneziano, Shounak Athavale, and Marta C  
569 González. The timegeo modeling framework for urban mobility without travel surveys. *Proceed-  
570 ings of the National Academy of Sciences*, 113(37):E5370–E5378, 2016.
- 571  
572 Woosuk Kwon, Zhuohan Li, Siyuan Zhuang, Ying Sheng, Lianmin Zheng, Cody Hao Yu, Joseph  
573 Gonzalez, Hao Zhang, and Ion Stoica. Efficient memory management for large language model  
574 serving with pagedattention. In *Proceedings of the 29th Symposium on Operating Systems Prin-  
575 ciples*, pp. 611–626, 2023.
- 576  
577 Ji Lin, Jiaming Tang, Haotian Tang, Shang Yang, Wei-Ming Chen, Wei-Chen Wang, Guangxuan  
578 Xiao, Xingyu Dang, Chuang Gan, and Song Han. Awq: Activation-aware weight quantization for  
579 on-device llm compression and acceleration. *Proceedings of Machine Learning and Systems*, 6:  
580 87–100, 2024.
- 581  
582 Douglas S Massey and Nancy A Denton. The dimensions of residential segregation. *Social forces*,  
583 67(2):281–315, 1988.
- 584  
585 Xupeng Miao, Gabriele Oliaro, Zhihao Zhang, Xinhao Cheng, Hongyi Jin, Tianqi Chen, and Zhihao  
586 Jia. Towards efficient generative large language model serving: A survey from algorithms to  
587 systems. *arXiv preprint arXiv:2312.15234*, 2023.
- 588  
589 Esteban Moro, Dan Calacci, Xiaowen Dong, and Alex Pentland. Mobility patterns are associated  
590 with experienced income segregation in large us cities. *Nature communications*, 12(1):4633,  
591 2021.
- 592  
593 Keivalya Pandya and Mehfuza Holia. Automating customer service using langchain: Building cus-  
594 tom open-source gpt chatbot for organizations. *arXiv preprint arXiv:2310.05421*, 2023.
- 595  
596 Joon Sung Park, Joseph O’Brien, Carrie Jun Cai, Meredith Ringel Morris, Percy Liang, and  
597 Michael S Bernstein. Generative agents: Interactive simulacra of human behavior. In *Proceedings  
598 of the 36th annual acm symposium on user interface software and technology*, pp. 1–22, 2023.
- 599  
600 Larry L Peterson and Bruce S Davie. *Computer networks: a systems approach*. Morgan Kaufmann,  
601 2007.

- 594 Chen Qian, Xin Cong, Cheng Yang, Weize Chen, Yusheng Su, Juyuan Xu, Zhiyuan Liu,  
595 and Maosong Sun. Communicative agents for software development. *arXiv preprint*  
596 *arXiv:2307.07924*, 6, 2023.
- 597 Thomas C Schelling. *Micromotives and macrobehavior*. WW Norton & Company, 2006.
- 599 Chenyang Shao, Fengli Xu, Bingbing Fan, Jingtao Ding, Yuan Yuan, Meng Wang, and Yong Li.  
600 Beyond imitation: Generating human mobility from context-aware reasoning with large language  
601 models. *arXiv preprint arXiv:2402.09836*, 2024.
- 602 Chaoming Song, Tal Koren, Pu Wang, and Albert-László Barabási. Modelling the scaling properties  
603 of human mobility. *Nature physics*, 6(10):818–823, 2010.
- 605 Lei Wang, Jingsen Zhang, Xu Chen, Yankai Lin, Ruihua Song, Wayne Xin Zhao, and Ji-Rong  
606 Wen. Recagent: A novel simulation paradigm for recommender systems. *arXiv preprint*  
607 *arXiv:2306.02552*, 2023.
- 608 Lei Wang, Chen Ma, Xueyang Feng, Zeyu Zhang, Hao Yang, Jingsen Zhang, Zhiyuan Chen, Jiakai  
609 Tang, Xu Chen, Yankai Lin, et al. A survey on large language model based autonomous agents.  
610 *Frontiers of Computer Science*, 18(6):186345, 2024.
- 612 Jason Wei, Xuezhi Wang, Dale Schuurmans, Maarten Bosma, Fei Xia, Ed Chi, Quoc V Le, Denny  
613 Zhou, et al. Chain-of-thought prompting elicits reasoning in large language models. *Advances in*  
614 *neural information processing systems*, 35:24824–24837, 2022.
- 615 Zhiheng Xi, Wenxiang Chen, Xin Guo, Wei He, Yiwen Ding, Boyang Hong, Ming Zhang, Junzhe  
616 Wang, Senjie Jin, Enyu Zhou, et al. The rise and potential of large language model based agents:  
617 A survey. *arXiv preprint arXiv:2309.07864*, 2023.
- 618 Fengli Xu, Jun Zhang, Chen Gao, Jie Feng, and Yong Li. Urban generative intelligence (ugi): A  
619 foundational platform for agents in embodied city environment. *arXiv preprint arXiv:2312.11813*,  
620 2023.
- 622 Hui Yang, Sifu Yue, and Yunzhong He. Auto-gpt for online decision making: Benchmarks and  
623 additional opinions. *arXiv preprint arXiv:2306.02224*, 2023.
- 624 John Yang, Carlos E Jimenez, Alexander Wettig, Kilian Lieret, Shunyu Yao, Karthik Narasimhan,  
625 and Ofir Press. Swe-agent: Agent-computer interfaces enable automated software engineering.  
626 *arXiv preprint arXiv:2405.15793*, 2024.
- 627 Lianmin Zheng, Liangsheng Yin, Zhiqiang Xie, Jeff Huang, Chuyue Sun, Cody Hao Yu, Shiyi Cao,  
628 Christos Kozyrakis, Ion Stoica, Joseph E Gonzalez, et al. Efficiently programming large language  
629 models using sglang. *arXiv preprint arXiv:2312.07104*, 2023.

## 632 A URBAN MOBILITY DATASET

634 As shown in Table A1, we collect urban mobility data of 6 major cities around the world. The  
635 data sources vary. In Beijing, the data is from a related work Shao et al. (2024), which gathered  
636 through a social network platform and tracking users’ mobility trajectories. Additionally, users’  
637 profiles, such as income level, gender, occupation, education level and age, are collected through  
638 digital surveys. In New York and San Francisco, the data comes from Safegraph, which provides  
639 aggregated population flow among Points of Interest (POIs) and Census Block Groups (CBGs). The  
640 other three cities—London, Paris and Sydney—use data are from Foursquare. Foursquare data  
641 consist of thousands of check-ins data of users and the corresponding venue position.

642 To make better use of the datasets, we apply several preprocessing methods. We firstly arrange the  
643 trajectory points in time sequence, and divide the trajectory into units of one day. Then we filter out  
644 trajectories with fewer than 4 points in a day, as they do not fully capture users’ mobility patterns.  
645 For home extraction, we identify the most frequently visited location of the users’ home. Since  
646 only the Tencent dataset includes user profiles, we make profile sampling for users of each city based  
647 on local census data for the other two datasets. In the end, our dataset is optimized for easy use in  
urban mobility simulations.

Source	City	Users	Trajectory Points	Duration
Shao et al. (2024)	Beijing	100000	297363263	Oct. 2019 - Dec. 2019
Safegraph	New York	Aggregated	760493	May 2023 - July 2023
	San Francisco	Aggregated	316732	
Foursquare	London	9409	173268	Apr. 2012 - Sept. 2013
	Paris	5809	85679	
	Sydney	1720	54170	

Table A1: Basic information about the dataset

## B URBAN DYNAMIC METRICS

We use comprehensive metrics in three-levels to evaluate the simulation performance, from individual-level to group level, and also from physical domain to social domain. These metrics allows us to gain a full understanding of mobility patterns and their implications, and can also help us evaluate the performance of the simulation by analysing the generated trajectory.

At the individual level, we calculate radius of gyration  $r_g$  Gonzalez et al. (2008) for each user, which is a measure of the spatial extent of their movements. The radius of gyration is defined as follows:

$$r_g^\alpha = \sqrt{\frac{1}{N^\alpha} \sum_{i=1}^{N^\alpha} (\vec{r}_i^{\alpha x} - \vec{r}_{cm}^{\alpha x})^2} \quad (3)$$

where  $\vec{r}_i^{\alpha x}$  represents the  $i = 1, 2, \dots, N$  positions recorded by user  $\alpha$ , and  $r_{cm}^\alpha = 1/N^\alpha \sum_{i=1}^{N^\alpha} (\vec{r}_i^{\alpha x})$  is the center of mass of the trajectory. The radius of gyration provides an indication of the size of a user’s activity range. To assess the accuracy of our simulation data against real-world data for a specific user, we calculate  $R_{MSE}$ , the Mean Squared Error(MSE) of the radius of gyration.

To analyze movement patterns and other aggregated features, we define block areas as spatial units within the city. For cities with Safegraph data, we use existing Census Block Group (CBG) areas. For other cities, we divide the map area into evenly spaced grids, with each grid cell representing a block area.

At the group level, we count the inflow and outflow of agents between block areas, calculate the Origin-Destination (OD) matrix Jiang et al. (2016), and normalize it. To compare real data with simulation data, we calculate the MSE of the normalized OD matrix, denoted as  $OD_{MSE}$ . A smaller  $OD_{MSE}$  value indicates greater similarity between the OD matrices, meaning the movement characteristics of the simulated data closely match the real data.

At the social domain, we calculate the income segregation index Moro et al. (2021) for each block area. The income segregation of a place  $\alpha$  is defined as  $S_\alpha = \frac{5}{8} \sum_q |\tau_{q\alpha} - \frac{1}{5}|$ , where  $\tau_{q\alpha}$  is the proportion of visitors in each income quintile for place  $\alpha$ . The  $S_\alpha$  ranges from 0 to 1. A high  $S_\alpha$  indicates that the place  $\alpha$  is predominantly visited by a single income group, suggesting a high level of income segregation. We denote  $S_{MSE}$  as the MSE between the real data and simulation data.

## C IMAGE SUPPLEMENTS

702  
703  
704  
705  
706  
707  
708  
709  
710  
711  
712  
713  
714  
715  
716  
717  
718  
719  
720  
721  
722  
723  
724  
725  
726  
727  
728  
729  
730  
731  
732  
733  
734  
735  
736  
737  
738  
739  
740  
741  
742  
743  
744  
745  
746  
747  
748  
749  
750  
751  
752  
753  
754  
755

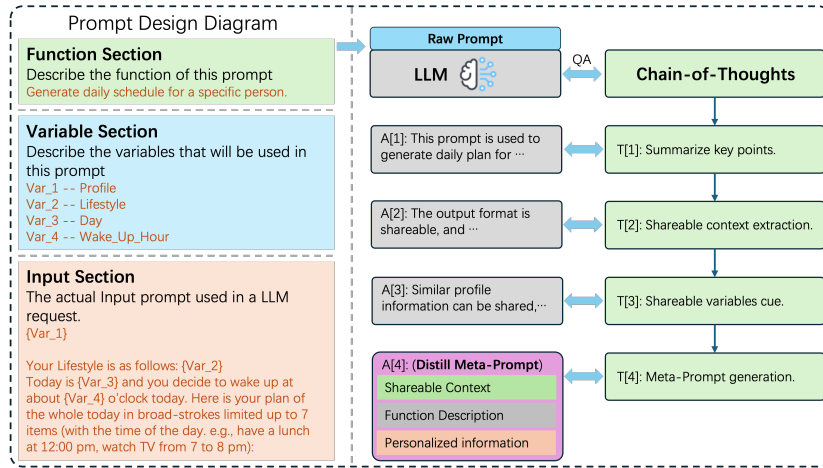


Figure A1: Distill meta-prompt generation through CoT inference.



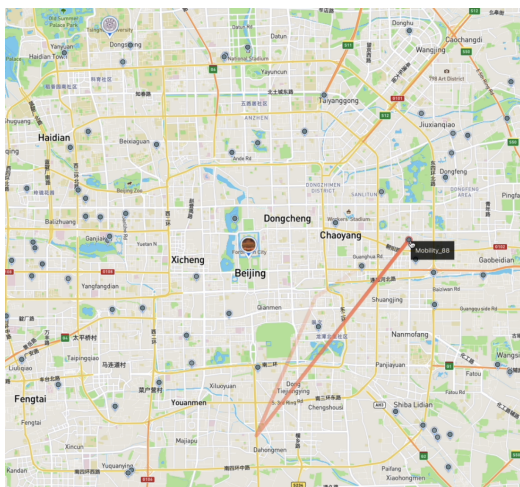
(a) Agent Construction

Citizen Profile (Beijing)

Minimum age: 20    Maximum age: 100    Gender: Female x    Education Level: PhD x Bachelor's x Bachelor's x    Consumption Level: Fairly High x    Refresh

Simulator ID	Gender	Age	Education Level	Consumption Level	Residence AOI	Action
96	Female	32	Bachelor's	Fairly High	富华行会议室	Bind
15	Female	55	PhD	Fairly High	中共中央办公厅秘书局	Bind
22	Female	23	Bachelor's	Fairly High	山景丽园(旺静里中街)	Bind

(b) Profile Configuration



(c) Simulation Visualization



(d) Result Visualization

Figure A2: Overview of OpenCity web portal.